JOURNAL OF THERMOPHYSICS AND HEAT TRANSFER
Vol. 15, No. 2, April–June 2001

Transport Coefficients for High-Temperature Nonequilibrium Air Flows

M. Fertig*
University of Stuttgart, 70550 Stuttgart, Germany
A. Dohr†
Technical University of Vienna, A-1040 Vienna, Austria
and
H.-H. Frühauf‡
University of Stuttgart, 70550 Stuttgart, Germany

A transport coefficient model based on the first approximation of the Chapman–Cowling theory was implemented into the URANUS nonequilibrium Navier–Stokes code to predict reentry flows more accurately. This model is compared to the widely used, simplified model of Gupta and Yos. The simplifications used to obtain the latter model are described in detail. The transport coefficients computed with both methods differ by up to a factor of two in the case of partially ionized air under equilibrium conditions. Therefore, the new model allows a more accurate description of the thermochemical relaxation in the shock region of significantly ionized, high-temperature flows. The differences in surface heat fluxes between the new model and the model of Yos and Gupta are smaller than 4%.

Nomenclature

$A^*, \ldots, I^*$	=	collision integral ratios
b	=	impact parameter
c_v	=	heat capacity
D	=	multicomponent diffusion coefficient
$\mathcal{D}$	=	binary diffusion coefficient
D_m	=	effective diffusion coefficient
D_m^a	=	effective ambipolar diffusion coefficient
D_m^T	=	thermal diffusion coefficient
d	=	mass diffusion driving force
E	=	energy
e	=	elementary charge
g	=	initial relative speed of a binary encounter, Eqs. (1) and (2); also degeneracy factor, Eqs. (52)–(54)
h	=	specific enthalpy
j	=	diffusion mass flux
k	=	Boltzmann constant
M	=	molar mass
$\bar{M}$	=	mixture molar mass
m	=	mass
n	=	number density
p	=	pressure
Q	=	partition function
R	=	gas constant
T	=	temperature
T^*	=	reduced temperature
u	=	specific energy
V	=	diffusion velocity
v	=	average velocity
X	=	external force
Z	=	number of charges
γ	=	reduced initial relative speed
$\Delta^{(l)}$	=	collision integral abbreviation
ε_0	=	permittivity of vacuum
η	=	viscosity
Θ	=	characteristic temperature
λ	=	heat conductivity
λ_D	=	Debye radius
μ	=	reduced mass
ν	=	number of species
ξ	=	mass fraction
ρ	=	density
φ	=	pressure fraction
χ	=	angle of deflection
ψ	=	molar fraction
$\bar{\Omega}_{ij}^{(l,s)}$	=	collision integral (average effective collision cross section)

Subscripts

CC	=	transport coefficients computed according to the Chapman–Cowling theory with the collision integrals of Capitelli et al.[10] and Mason et al.[11]
e	=	electron
el	=	electronic excitation
i, j	=	species indices
int	=	internal degree of freedom
mix	=	mixture
rot	=	rotational excitation
tr	=	heavy particle translation
trans	=	translational degrees of freedom
vib	=	vibrational excitation
YC	=	transport coefficients computed according to Yos's[9] simplified model with the collision integrals of Capitelli et al.[10] and Mason et al.[11]
YG	=	transport coefficients computed according to Yos's[9] simplified model with the collision integrals of Gupta et al.[4]

Introduction

IN recent years, great progress has been made in computing hypersonic nonequilibrium flows around reentry vehicles. Many efforts have been made to improve thermochemical relaxation models[1,2] and gas–surface interaction models accounting for finite catalycity.[3] However, the transport properties viscosity, heat conduction, and mass diffusion are more often than not computed with widely simplified formulas.[4] To improve the prediction of reentry

Received 23 February 2000; revision received 6 July 2000; accepted for publication 27 July 2000.

*Ph.D. Student, Institut für Raumfahrtsysteme, Pfaffenwaldring 31, D.
†Student, Rögergasse 4, A 1090 Wien, Austria.
‡Senior Scientist, Institut für Raumfahrtsysteme, Pfaffenwaldring 31, D. Member AIAA.

flows, Chapman–Cowling formulas have been implemented into the fully coupled, fully implicit, 11-species, 6-temperature nonequilibrium Navier–Stokes code URANUS.[5,6]

The Chapman–Cowling method was developed from rigorous kinetic gas theory and relates the transport coefficients to the pair potential energy functions of the particles in the gas. The potential energy functions are used to determine the so-called collision integrals. The transport coefficients of monoatomic gases are then approximated by an infinite series in terms of the collision integrals. The number of elements of this series that are taken into account determines the approximation level. It was shown by Devoto[7] that, especially in case of ionized gases, the accuracy of the second approximation of the heat conductivity is low. In the fully ionized limit of hydrogen, Devoto computed heat conductivities differing by 57% between the second and the third approximation. He concluded that at least the next higher level of approximation has to be used for ionized gases to obtain the correct transport coefficients. Because the computation of the higher approximations for a multicomponent mixture is extremely laborious, Devoto separated the Boltzmann equations for the heavy particles and for the electrons.[8] Unfortunately, no accurate measurement of heat conductivities for air can be found in literature for temperatures higher than 15,000 K because at higher temperatures plasma radiation influences the determination of the transport properties. Therefore, the only way to determine the accuracy of the computed transport coefficients is the comparison of the results of different models with different accuracy.

As already mentioned, the determination of the higher levels of approximation to the transport coefficients requires not only a lot of computational work, but also the knowledge of many additional collision integrals. The influence of the transport coefficients onto reentry nonequilibrium flows is, therefore, investigated comparing the low levels of approximation of the Chapman–Cowling theory with the simplified models of Gupta et al.[4] and Yos.[9]

The collision integrals from Gupta et al.[4] do not differ much from those given by Yos.[9] Hence, the collision integrals have been updated with those recently published by Capitelli et al.[10] Because the Capitelli et al. publication contains only interactions with neutral particles, the shielded coulomb collision integrals from Mason et al.[11] have been used for the charged species interactions.

Collision Integrals

The transport coefficients used in the conservation equations of the nonequilibrium Navier–Stokes code URANUS[6] can be expressed in terms of the collision integrals.[12] To obtain the collision integrals from the interaction potentials for two colliding particles, three subsequent integrations have to be performed. Because of the large computational work needed, this can not be done during a flowfield simulation. Therefore, similar to Gupta et al.,[4] the averaged collision integrals $\bar{\Omega}_{ij}^{(1,1)}$ and $\bar{\Omega}_{ij}^{(2,2)}$ were fitted. The underlying collision integrals are defined by

$$\Omega_{ij}^{(l,s)}(T_i, T_j) = \frac{8\pi(l+1)}{(s+1)![2l+1-(-1)^l]} \cdot \int_0^\infty \int_0^\infty e^{-\gamma^2} \gamma^{2s+3} [1-\cos^l \chi(b,g)] b \, \mathrm{d}b \, \mathrm{d}\gamma \tag{1}$$

where the angle of deflection $\chi(b, g)$ and the initial relative speed g have the usual meaning as defined by Hirschfelder et al.[12] In case of different translational temperatures of the species i and j, the reduced initial relative speed has to be defined by

$$\gamma_{ij} = \sqrt{\frac{\mu_{ij} g_{ij}^2}{2kT_{ij}}} \tag{2}$$

with the reduced mass and the mass averaged temperature

$$\mu_{ij} = \frac{m_i m_j}{m_i + m_j}, \qquad T_{ij} = \frac{m_i T_j + m_j T_i}{m_i + m_j} \tag{3}$$

If only one heavy particle translational temperature and an electron temperature are considered, the mass averaged temperatures may be simplified such that

$$T_{ij} = T_{\mathrm{tr}}, \qquad \text{if} \quad i \neq e \quad \text{and} \quad j \neq e \tag{4}$$

$$T_{ie} \approx T_e \tag{5}$$

The interactions between ionized species are assumed to depend on electrostatic forces shielded by the Debye radius

$$\lambda_D = \sqrt{\frac{\varepsilon_0 k}{e^2}\left(\frac{n_e}{T_e} + \sum_{i=\mathrm{Ion}} \frac{Z_i^2}{T_i} n_i\right)^{-1}} \tag{6}$$

For this reason, the collision integrals of the ionized species are computed by the formula

$$\bar{\Omega}_{ij}^{(l,s)}(T_i, T_j) = \pi \left(\lambda_D / T_{ij}^*\right)^2 \Omega_{ij}^{(l,s)*}\left(T_{ij}^*\right) \tag{7}$$

from the dimensionless collision integrals given by Mason et al.[11] with the dimensionless temperature

$$T_{ij}^* = \lambda_D \left(e^2 / 4\pi\varepsilon_0 k T_{ij}\right)^{-1} \tag{8}$$

Note that the collision integrals used here have the dimension of a collision cross section and differ, therefore, by a factor of the rigid sphere collision cross section $\pi\sigma^2$ from the definition of the dimensionless $\Omega^{(l,s)*}$ given by Hirschfelder et al.[12] To simplify the equations given hereafter, we introduce the abbreviations

$$\Delta_{ij}^{(1)} = \tfrac{8}{3}\sqrt{2\mu_{ij}/\pi k T_{ij}}\,\bar{\Omega}_{ij}^{(1,1)}, \qquad \Delta_{ij}^{(2)} = \tfrac{16}{5}\sqrt{2\mu_{ij}/\pi k T_{ij}}\,\bar{\Omega}_{ij}^{(2,2)} \tag{9}$$

and the cross section ratios

$$A_{ij}^* = \bar{\Omega}_{ij}^{(2,2)} / \bar{\Omega}_{ij}^{(1,1)}, \qquad B_{ij}^* = \left(5\bar{\Omega}_{ij}^{(1,2)} - 4\bar{\Omega}_{ij}^{(1,3)}\right) / \bar{\Omega}_{ij}^{(1,1)} \tag{10}$$

Diffusion

Mass diffusion is the main energy transport mechanism in boundary layers at highly catalytic surfaces. For flow cases with a high degree of dissociation in the boundary layer, the heat fluxes calculated for non- and fully catalytic surfaces will differ by more than a factor of two.[3] Diffusion occurs in a mixture if the relative velocities of the individual species do not vanish. Summation of the species average velocities $\bar{v}_i$ multiplied with the mass partial densities ρ_i and divided by the overall density of the mixture gives the mass average velocity

$$v = \sum_{i=1}^{\nu} \xi_i \bar{v}_i \tag{11}$$

of the mixture. Now it is possible to define the diffusion velocity

$$\bar{V}_i = \bar{v}_i - v \tag{12}$$

From Eqs. (11) and (12) it follows that

$$\sum_{i=1}^{\nu} \rho_i \bar{V}_i = \sum_{i=1}^{\nu} j_i = 0 \tag{13}$$

Following Hirschfelder et al.,[12] $\boldsymbol{j}_i$ is given by

$$\boldsymbol{j}_i = \frac{\rho}{\bar{M}^2} \sum_{j=1}^{\nu} M_i M_j D_{ij} \boldsymbol{d}_j - \frac{D_i^T}{T} \nabla T \tag{14}$$

with

$$\boldsymbol{d}_j = \nabla \varphi_j + \frac{\varphi_j - \xi_j}{p} \nabla p - \frac{1}{p}\left[n_j \boldsymbol{X}_j - \xi_j \sum_{k=1}^{\nu} n_k \boldsymbol{X}_k\right] \tag{15}$$

where $\varphi_i = p_i / p$ are the pressure fractions and $\boldsymbol{X}_i$ and $\boldsymbol{X}_k$ are external forces acting on the different species. Note that the evaluation of Eq. (14) requires the calculation of the multicomponent diffusion

coefficients [$\nu \cdot (\nu - 1)$ coefficients, where every coefficient requires the solution of $\nu + 1$ coupled equations], which is quite a cumbersome task. If we restrict ourselves dealing with no more than the first approximation of the theory of Chapman and Cowling, Hirschfelder et al.[12] have shown that Eq. (14) may be "turned wrong-side out" to obtain $\nu - 1$ independent relations

$$\sum_{j=1}^{\nu} \frac{\psi_i \psi_j}{\mathcal{D}_{ij}} \left(\frac{\boldsymbol{j}_j}{\rho_j} - \frac{\boldsymbol{j}_i}{\rho_i} \right) = \boldsymbol{d}_i - \frac{1}{T} \sum_{j=1}^{\nu} \frac{\psi_i \psi_j}{\mathcal{D}_{ij}} \left(\frac{D_j^T}{\rho_j} - \frac{D_i^T}{\rho_i} \right) \nabla T \tag{16}$$

with the first-order binary diffusion coefficients

$$\mathcal{D}_{ij} = \frac{3}{16} \frac{\sqrt{2\pi k^3 T^3}}{p \bar{\Omega}_{ij}^{(1,1)} \sqrt{\mu_{ij}}} = \mathcal{D}_{ji} \tag{17}$$

Equations (16) and (17) have been developed for thermal equilibrium and should be replaced by the generalized equations of Ramshaw and Chang[13] if the electron temperature is much higher than the heavy particle temperature. In this paper the assumption was made that thermal diffusion is negligible; hence, no expression will be given for D_i^T. Equation (16) together with Eq. (13) constitute a system of ν independent relations of the form

$$\bar{\bar{K}} \cdot \boldsymbol{j} = \boldsymbol{d} \tag{18}$$

which can be solved directly for the diffusion mass fluxes $\boldsymbol{j} = (j_{x,i}, j_{y,i}, j_{z,i})$ without evaluation of the D_{ij}.

Ambipolar Diffusion

In case of ionization, charge neutrality is required in the bulk gas, leading to

$$\sum_{i=1}^{\nu} Z_i n_i = 0, \qquad \sum_{i=1}^{\nu} Z_i n_i \bar{V}_i = 0 \tag{19}$$

Because the electrons and the ions tend to diffuse with different velocities, a charge separation occurs, setting up an ambipolar electric field. Similar to the work of Devoto,[7] an ambipolar electric field was introduced as an external force into the diffusion force of Eq. (15) and solved for Eq. (19). This changes the elements D_{ij}^* of the inverted matrix $\bar{\bar{K}}^{-1}$ in Eq. (18) to

$$D_{ij}^{*a} = D_{ij}^* + \frac{\sum_{k=1}^{\nu} Z_k D_{ik}^* \psi_k}{\sum_{l=1}^{\nu} \sum_{m=1}^{\nu} Z_l Z_m D_{lm}^* \psi_m} \cdot \sum_{n=1}^{\nu} Z_n D_{nj}^* \tag{20}$$

Because the electric field accelerates all of the charged particles depending on Z_i, the diffusion velocity of the electrons is especially changed to fulfill Eq. (19) due to the relatively small momentum of the electrons.

Simplified Diffusion Model

Yos[9] gives an equation similar to Fick's law for multicomponent mixtures:

$$\boldsymbol{j}_i' = -\rho D_{im} \nabla \psi_i \tag{21}$$

Based on Eq. (16), such a simplification can be achieved by assuming that $\bar{V}_j = \text{const}$ for $j \neq i$, $T_i = T_j$, and by neglecting all but the first term in Eq. (15). Using Eq. (13) to connect $\bar{V}_i$ and $\bar{V}_j$, one finds

$$D_{im} = \frac{M_i (1 - \xi_i)}{\bar{M} \sum_{\substack{j=1 \\ j \neq i}}^{\nu} (\psi_j / \mathcal{D}_{ij})} \tag{22}$$

$$\boldsymbol{d}_i \approx \nabla (n_i k T_i / p) \approx \nabla (n_i / n) = \nabla \psi_i \tag{23}$$

An equation similar to Eq. (20) is meaningless in the case of effective diffusion coefficients because the charge neutrality from Eq. (19) as well as the mass conservation from Eq. (13) are in error. Additionally, the computed diffusion fluxes are much too small. Therefore, we use Lee's[14] estimate that effective ambipolar diffusion coefficients have the double value of an effective ionic diffusion coefficient, that is,

$$D_{\text{Ion},m}^a \approx 2 D_{\text{Ion},m} \tag{24}$$

The heavy particles' diffusion fluxes are then computed from Eq. (21) and the electron diffusion fluxes from charge neutrality

$$j_e = \sum_{i=1 i \neq e}^{\nu} Z_i \frac{M_e}{M_i} j_i \tag{25}$$

Finally, the effective diffusion fluxes are corrected by

$$j_i \approx j_i' - \frac{|j_i'|}{\sum_{i=1}^{\nu} |j_i'|} \sum_{i=1}^{\nu} j_i' \tag{26}$$

to conserve mass. The more accurate flux correction (which was not used in our computations)

$$j_i = j_i' - \xi_i \sum_{j=1}^{\nu} j_i' \tag{27}$$

given by Sutton and Gnoffo,[15] improves the diffusion fluxes.

Viscosity

Another transport coefficient needed in Navier–Stokes calculations is the coefficient of viscosity, which is used to describe the shear forces and, therefore, the transport of momentum in the case of velocity gradients. Following Hirschfelder et al.,[12] one can express the viscosity of the mixture by $\nu + 1$ independent equations:

$$\sum_{j=1}^{\nu} H_{ij} \left(\frac{nkT_j}{2} b_{j0} \right) = \psi_i, \qquad \sum_{j=1}^{\nu} \psi_j \left(\frac{nkT_j}{2} b_{j0} \right) = [\eta_{\text{mix}}]_1 \tag{28}$$

where n is the overall particle number density, the b_{j0} are the Sonine coefficients used by Hirschfelder et al.,[12] and $[\eta_{\text{mix}}]_1$ is the first approximation to the coefficient of viscosity of a mixture. With the definitions from Eqs. (9) and (10) one finds from the Hirschfelder et al. formulas

$$H_{ii} = \frac{\psi_i^2}{m_i} \Delta_{ii}^{(2)} + \sum_{\substack{j=1 \\ j \neq i}}^{\nu} \frac{\psi_i \psi_j}{m_i + m_j} \Delta_{ij}^{(2)} \left[\frac{5}{3 A_{ij}^*} + \frac{m_j}{m_i} \right] \tag{29}$$

$$H_{ij} = \frac{\psi_i \psi_j}{m_i + m_j} \Delta_{ij}^{(2)} \left[1 - \frac{5}{3 A_{ij}^*} \right], \qquad i \neq j \tag{30}$$

Equations (28) can be solved for $[\eta_{\text{mix}}]_1$ by Cramer's rule as proposed by Hirschfelder et al.[12] or by LU decomposition. If $A_{ij}^* = \frac{5}{3}$, the off-diagonal elements H_{ij}, $j \neq i$ vanish and one obtains the approximate formula

$$[\eta_{\text{mix}}]_{1,y} = \sum_{i=1}^{\nu} \frac{\psi_i^2}{H_{ii}} = \cdots = \sum_{i=1}^{\nu} \frac{m_i \psi_i}{\sum_{j=1}^{\nu} \psi_j \Delta_{ij}^{(2)}} \tag{31}$$

given by Yos,[9] which is widely used in multicomponent Navier–Stokes calculations.

Thermal Conductivity

The last effect one has to deal with is heat conduction caused by temperature gradients. The transport coefficients used to describe this phenomenon are the coefficients of thermal conductivity.

Translational Degrees of Freedom

Until this point, the first step is the calculation of the coefficient of thermal conductivity for a mixture with all internal degrees of freedom considered frozen, that is, the mixture behaves like a mixture of monoatomic gases. This requires the assumption that the partition function of the particles can be expressed as a power series of partition functions for each kind of independent energy (see Vincenti and Kruger[16]). Formulas for this purpose have also been derived by Hirschfelder et al.[12] Unfortunately, the Hirschfelder et al. lowest-order formulas require the solution of not only $2\nu + 1$ equations, but also knowledge of the thermal diffusion coefficients. Hence, these formulas involve extremely laborious numerical computations. Therefore, the formulas given by Brokaw[17] are preferred. Brokaw's equations can be derived from the Hirschfelder et al.[12] formulas by assuming vanishing thermal diffusion as was done in the section "Diffusion". As in the preceding section, one obtains a set of $\nu + 1$ equations

$$\sum_{j=1}^{\nu} L_{ij}^{11}\left(\frac{5}{4}n\sqrt{\frac{2k^3T_j}{m_j}}a_{j1}\right) = -\psi_i$$

$$\sum_{j=1}^{\nu} \psi_j\left(\frac{5}{4}n\sqrt{\frac{2k^3T_j}{m_j}}a_{j1}\right) = -[\lambda_{\mathrm{mix,trans}}]_2 \tag{32}$$

where a_{j1} are the Sonine coefficients of Hirschfelder et al.[12] Expressing the L_{ij}^{11} in terms of Eqs. (9) and (10) one derives

$$L_{ii}^{11} = \frac{\psi_i}{k}\left\{\frac{4}{15}\psi_i\Delta_{ii}^{(2)} + \sum_{\substack{k=1\\k\neq i}}^{\nu}\frac{\psi_k\Delta_{ik}^{(1)}}{(m_i+m_k)^2}\left[\frac{16}{25}A_{ik}^* m_i m_k + \left(1 - \frac{12}{25}B_{ik}^*\right)m_k^2 + \frac{6}{5}m_i^2\right]\right\}$$

and for $i \neq j$

$$L_{ij}^{11} = \frac{\psi_i}{k}\left\{\frac{\psi_i\mu_{ij}}{m_i+m_j}\Delta_{ij}^{(1)}\left(\frac{16}{25}A_{ij}^* + \frac{12}{25}B_{ij}^* - \frac{11}{5}\right)\right\} \tag{33}$$

Again, the Eqs. (32) can be solved for $[\lambda_{\mathrm{mix,trans}}]_1$ by Cramer's rule or by LU decomposition. To obtain separate equations for the thermal conductivity of the electrons and of the heavy particles, it is necessary to perform backward substitution in the system of Eqs. (32) to derive the Sonine coefficient of the electrons with the same level of approximation:

$$[\lambda_{\mathrm{mix},e}]_2 = -\tfrac{5}{4}\psi_e n\sqrt{2k^3T_e/m_e}\,a_{e1} \tag{34}$$

$$[\lambda_{\mathrm{mix,tr}}]_2 = [\lambda_{\mathrm{mix,trans}}]_2 - [\lambda_{\mathrm{mix},e}]_2 \tag{35}$$

As mentioned in the Introduction, the lowest approximation to the translational thermal conductivity is not able to give the transport coefficients sufficiently accurate in the case of ionized gases. Devoto showed[8] that the accuracy can be improved if the electron thermal conductivity is computed with a higher level of approximation while the coupling terms between the electrons and the heavy particles are neglected. Therefore, the heavy particles' thermal conductivity is computed according to Eq. (32). The electrons' thermal conductivity is determined with a higher level of approximation. The electron thermal conductivity then reads

$$[\lambda_{\mathrm{mix},e}]_3 = \psi_e^2\Big/\left[L_{ee}^{11} + \frac{\left(L_{ee}^{12}\right)^2}{L_{ee}^{22}}\right] \tag{36}$$

To evaluate Eq. (36), the additional collision terms

$$L_{ee}^{12} \approx \frac{\psi_e}{k}\left\{\psi_e\Delta_{ee}^{(2)}\left(\frac{7}{15} - \frac{8}{15}E_{ee}^*\right) + \sum_{\substack{k=1\\k\neq e}}^{\nu}\psi_k\Delta_{ek}^{(1)}\left[\frac{7}{4} - \frac{57}{25}B_{ek}^* + \frac{51}{10}C_{ek}^* - \frac{24}{5}G_{ek}^*\right]\right\}$$

$$L_{ee}^{22} \approx \frac{\psi_e}{k}\left\{\psi_e\Delta_{ee}^{(2)}\left(\frac{77}{60} - \frac{28}{15}E_{ee}^* + \frac{4}{3}H_{ee}^*\right) + \sum_{\substack{k=1\\k\neq e}}^{\nu}\psi_k\Delta_{ek}^{(1)}\left[\frac{49}{16} - \frac{399}{50}B_{ek}^* + \frac{126}{5}C_{ek}^* - \frac{168}{5}G_{ek}^* + \frac{72}{5}I_{ek}^*\right]\right\} \tag{37}$$

where the additional cross section ratios

$$C_{ij}^* = \frac{\bar{\Omega}_{ij}^{(1,2)}}{\bar{\Omega}_{ij}^{(1,1)}}, \qquad G_{ij}^* = \frac{\bar{\Omega}_{ij}^{(1,4)}}{\bar{\Omega}_{ij}^{(1,1)}}, \qquad I_{ij}^* = \frac{\bar{\Omega}_{ij}^{(1,5)}}{\bar{\Omega}_{ij}^{(1,1)}}$$

$$E_{ij}^* = \frac{\bar{\Omega}_{ij}^{(2,3)}}{\bar{\Omega}_{ij}^{(2,2)}}, \qquad H_{ij}^* = \frac{\bar{\Omega}_{ij}^{(2,4)}}{\bar{\Omega}_{ij}^{(2,2)}} \tag{38}$$

have been used. As can be seen from Eq. (33) a simple formula like Eq. (31) can be obtained by inserting the very unrealistic values of $A_{ij}^* = B_{ij}^* \approx \frac{55}{28} \approx 1.964$. A more accurate simplification can be found by rewriting Eqs. (32) by Cramer's rule as was done by Hirschfelder et al.[12] and expanding the ratio of determinants

$$[\lambda_{\mathrm{mix,trans}}]_2 = \sum_{i=1}^{\nu}\frac{\psi_i}{L_{ii}^{11}} - \sum_{i=1}^{\nu}\sum_{\substack{j=1\\j\neq i}}^{\nu}\frac{\psi_i\psi_j L_{ij}^{11}}{L_{ii}^{11}L_{jj}^{11}} + \sum_{i=1}^{\nu}\sum_{\substack{j=1\\j\neq i}}^{\nu}\sum_{\substack{k=1\\k\neq i}}^{\nu}\frac{\psi_i\psi_k L_{ij}^{11}L_{ik}^{11}}{L_{ii}^{11}L_{jj}^{11}L_{kk}^{11}} - \cdots \tag{39}$$

Brokaw[17] replaced this expansion by the approximate expression

$$[\lambda_{\mathrm{mix,trans}}]_2 \approx \sum_{i=1}^{\nu}\frac{\psi_i^2}{L_{ii}^{11}}\frac{1}{1+\sum_{i=1}^{\nu}\sum_{\substack{j=1\\j\neq i}}^{\nu}\left(L_{ij}^{11}/L_{jj}^{11}\right)(\psi_j/\psi_i)} = \sum_{i=1}^{\nu}\frac{\psi_i^2}{L_{ii}^{11}+\sum_{\substack{j=1\\j\neq i}}^{\nu}L_{ij}^{11}}\frac{1+\sum_{\substack{j=1\\j\neq i}}^{\nu}\left(L_{ij}^{11}/L_{ii}^{11}\right)}{1+\sum_{\substack{j=1\\j\neq i}}^{\nu}\left(L_{ij}^{11}/L_{jj}^{11}\right)(\psi_j/\psi_i)} \tag{40}$$

which agrees with Eq. (39) in the first three terms. Because the values of the off-diagonal elements L_{ij}^{11}, $i \neq j$, are small compared to the values of the L_{ii}^{11}, the last fraction is only a correction term close to unity and may, therefore, be neglected. Rearrangement leads to

$$[\lambda_{\mathrm{mix,trans}}]_2 \approx \sum_{i=1}^{\nu}\frac{\psi_i^2}{L_{ii}^{11}+\sum_{\substack{j=1\\j\neq i}}^{\nu}L_{ij}^{11}} = \cdots = \frac{15k}{4}\sum_{i=1}^{\nu}\frac{\psi_i}{\sum_{j=1}^{\nu}\alpha_{ij}\psi_j\Delta_{ij}^{(2)}} \tag{41}$$

where

$$\alpha_{ij} = \left(\frac{m_i}{m_j} - 1\right)\left[\left(\frac{3}{2}\frac{B^*_{ij}}{A^*_{ij}} - \frac{25}{8A^*_{ij}} + 1\right) + \left(\frac{15}{4A^*_{ij}} - 1\right)\frac{m_i}{m_j}\right] \Bigg/ \left(1 + \frac{m_i}{m_j}\right)^2 \tag{42}$$

Inserting the empirical values for air $A^*_{ij} = B^*_{ij} \approx 1.06$ finally gives a parameter

$$\alpha'_{ij} = 1 + \frac{(1 - m_i/m_j)[0.45 - 2.54(m_i/m_j)]}{(1 + m_i/m_j)^2} \tag{43}$$

which only depends on the species' masses.

The approximate thermal conductivity formula for air given by Yos[9] may be obtained by replacing α_{ij} in Eq. (41) by α'_{ij}. Separating the equation for the overall translational thermal conductivity into two independent parts for the heavy particles and the electrons then gives

$$[\lambda_{\mathrm{mix,tr}}]_{2,y} = \frac{15k}{4}\sum_{\substack{i=1\\ i\neq e}}^{\nu} \frac{\psi_i}{\sum_{j=1}^{\nu} \alpha'_{ij}\psi_j \Delta^{(2)}_{ij}} \tag{44}$$

$$[\lambda_{\mathrm{mix},e}]_{2,y} = \frac{15k}{4}\frac{\psi_e}{\sum_{j=1}^{\nu} \alpha'_{ij}\psi_j \Delta^{(2)}_{ij}} \tag{45}$$

Note, that the accuracy for ionized gases can be significantly improved if Eq. (45) is replaced by Eq. (36).

Internal Degrees of Freedom

Heat conduction of internal degrees of freedom can not be directly obtained by the Chapman–Cowling method because the collision integrals do not account for the internal structure of the colliding species. Brokaw[17] gives an approximate formula, based on an Eucken correction, which accounts for the transport of internal energy by a diffusion mechanism

$$\lambda_{\mathrm{mix,int}} = \sum_i \frac{[\lambda_{\mathrm{int},i}]_1}{1 + \sum_{j\neq i}(\mathcal{D}_{ii}/\mathcal{D}_{ij})(\psi_j/\psi_i)} \tag{46}$$

In this expression $\lambda_{\mathrm{int},i} = c_{v,\mathrm{int},i}[\eta_i]_1$ is the Eucken correction term for a single species. Rearrangement of Eq. (46) leads to

$$\lambda_{\mathrm{mix,int}} = k\sum_i \frac{(c_{v,\mathrm{int},i}/R_i)\left(5/6A^*_{ii}\right)\psi_i}{\sum_j \Delta^{(1)}_{ij}\psi_j} \tag{47}$$

which differs from Yos's[9] formulas by the fraction $5/6A^*_{ii}$, which is a value close to unity for oxygen and nitrogen molecules. Referring to Vincenti and Kruger,[16] the specific heat capacities of the internal degrees of freedom may be obtained by the equations

$$u_{\mathrm{int},i} = R_i T^2 \frac{\partial}{\partial T}\ell n\, Q_{\mathrm{int},i} \tag{48}$$

$$c_{v,\mathrm{int},i} = \left(\frac{\partial u_{\mathrm{int},i}}{\partial T}\right)_v \tag{49}$$

If the assumption is made that the rotational degree of freedom may be modeled by a rigid rotator truncated at the dissociation energy, one gets

$$c_{v,\mathrm{rot},i} = R_i\left\{1 - \left[\frac{\Theta_{D,i}/2T_{\mathrm{rot},i}}{\sinh(\Theta_{D,i}/2T_{\mathrm{rot},i})}\right]^2\right\} \tag{50}$$

An appropriate model for the description of vibrational excitation is a truncated harmonic oscillator, which leads to

$$c_{v,\mathrm{vib},i} = R_i\left\{\left[\frac{\Theta_{\mathrm{vib},i}/2T_{\mathrm{vib},i}}{\sinh(\Theta_{\mathrm{vib},i}/2T_{\mathrm{vib},i})}\right]^2 - \left[\frac{\Theta_{D,i}/2T_{\mathrm{vib},i}}{\sinh(\Theta_{D,i}/2T_{\mathrm{vib},i})}\right]^2\right\} \tag{51}$$

where the second term describes the truncation at the dissociation energy $E_{D,i} = \Theta_{D,i}/R_i$. This term has the effect that the specific rotational and vibrational heat capacity of the molecules will decrease at high temperatures due to the limited number of energy levels. Electronic excitation, finally, may be described by a subsequent set of excitation levels

$$Q_{\mathrm{el},i} = \sum_{k=0}^{k_{\max}} g_{k,i}\exp\left(-\frac{\Theta_{\mathrm{el},k,i}}{T_{\mathrm{el}}}\right) \tag{52}$$

Evaluating the specific energy of electronic excitation, one obtains

$$e_{\mathrm{el},i} = \frac{R_i}{Q_{\mathrm{el},i}}\sum_{k=0}^{k_{\max}} g_{k,i}\Theta_{\mathrm{el},k,i}\exp\left(-\frac{\Theta_{\mathrm{el},k,i}}{T_{\mathrm{el}}}\right) \tag{53}$$

The specific heat capacity may then be expressed in terms of Eqs. (52) and (53) as

$$c_{v,\mathrm{el},i} = \frac{R_i}{T^2_{\mathrm{el}}}\left[\frac{\sum_{k=0}^{k_{\max}} g_{k,i}\Theta^2_{\mathrm{el},k,i}\exp(-\Theta_{\mathrm{el},k,i}/T_{\mathrm{el}})}{Q_{\mathrm{el},i}} - \left(\frac{e_{\mathrm{el},i}}{R_i}\right)^2\right]^2 \tag{54}$$

Another way to derive the thermal conductivities was used by Pascal and Brun.[18] They give equations for the translational and internal conductivities for a two-component mixture, taking into account the coupling of translational, rotational, and vibrational degrees of freedom. Because the computed differences compared to the results of the equations presented here are small in thermal equilibrium as well as in nonequilibrium, the coupling terms are expected to be negligible.

Equilibrium Results

Because calculated transport coefficients in thermal and chemical nonequilibrium strongly depend on the gas-phase and the gas–surface model, the first validation step of the new transport coefficient model is the check in local thermal and chemical equilibrium. In this case, one may define so called heat conductivities due to chemical reactions

$$\lambda_{\mathrm{react}} \approx -\sum_{i=1}^{\nu} h_i \frac{\partial j_i}{\partial T} \tag{55}$$

which allow one to give equations for the overall thermal conductivities

$$\lambda_{\mathrm{tot}} \equiv \lambda_{\mathrm{mix,tr}} + \lambda_{\mathrm{mix},e} + \lambda_{\mathrm{mix,rot}} + \lambda_{\mathrm{mix,vib}} + \lambda_{\mathrm{mix,el}} + \lambda_{\mathrm{mix,react}} \tag{56}$$

where effects due to radiation have been neglected.

Figure 1 shows the overall heat conductivies computed with the present model and the Capitelli et al.[10] collision integrals (CC), Yos's[9] model and the Capitelli et al.[10] collision integrals (YC), and with Yos's[9] model and the Gupta et al.[4] collision integrals (YG) together with experimental data (see also Ref. 19). Very good agreement is shown for low temperatures. Depending on the collision integrals used, significant differences arise at about 3800 and 7000 K. The local maxima of the total thermal conductivity at these temperatures depend on oxygen dissociation (3800 K) and on nitrogen dissociation (7000 K). However, if the Capitelli et al.[10] collision integrals are used, the different models for the transport coefficients

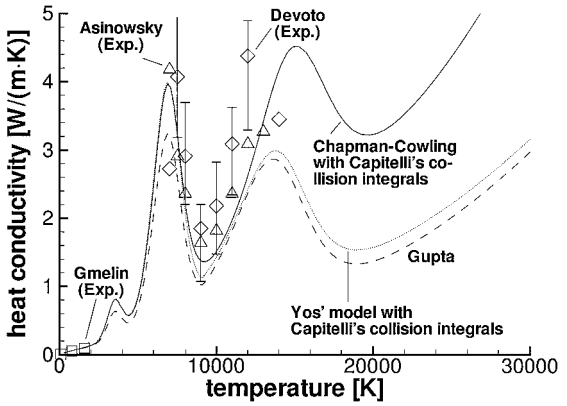

Fig. 1 Total heat conductivity for air at $p = 1$ bar vs temperature: solid line, present model with Capitelli et al.[10] collision integrals (CC); dashed line, simplified models with Gupta et al.[4] collision integrals (YG); and dotted line; simplified models with Capitelli et al.[10] collision integrals (experimental results are taken from Gmelin[19] and Devoto et al.[20]).

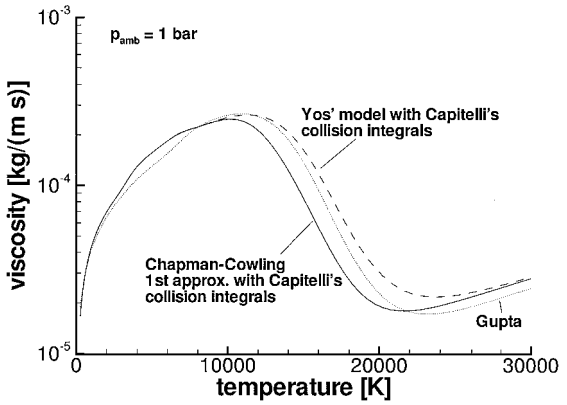

Fig. 2 Mixture viscosity for air at $p = 1$ bar vs temperature.

are close together and show a very good agreement with experimental data.

If the temperature exceeds 8000 K, differences of the transport coefficient models can be observed that rise with temperature. The formulas presented here are in good agreement with the experimental data of Asinowsky (see Ref. 20) whereas the experimental findings of Devoto et al.[20] are much higher beyond 10000 K. Devoto et al. expected that the discrepancies at elevated temperatures are caused by plasma radiation. When mass diffusion and electron thermal conductivity are depended on, the simplified Yos's[9] model predicts about 50% lower total thermal conductivities in comparison to the present one.

On the one hand, the collision integrals of the ionized species are very different from the neutral ones. On the other hand, the molar mass of the electrons is several orders of magnitude smaller than the molar masses of the heavy particles. Therefore, the assumption of identical diffusion velocities of all species, which is necessary to determine the effective diffusion coefficients, is invalid and leads to the significant error. In addition, the third approximation of the electron thermal conductivity is about two times the value of the simplified formula.

Mixture viscosity is shown in Fig. 2. The plot shows that the computed mixture viscosity values agree well for dissociated air. In the case of partial ionization at about 16,000 K, the simplified model's mixture viscosity differs by more than a factor of two compared to the value of the Chapman–Cowling first approximation. The differences compared to the Gupta et al.[4] model for fully ionized air (above 26,000 K) is a result of the different collision integrals for charged species interactions.

Note that the equilibrium results given here have been included for further reference to explain differences in the nonequilibrium discussion. They may be compared with the results of Bacri and Raffanel[21] or Murphy and Arundell.[22] Although the CC results compare well with those given there,[21,22] differences arise, especially for very high temperatures, because multiple ionization is neglected. These differences mainly depend on the 11-species air model used in the nonequilibrium scheme URANUS (N_2, O_2, NO, N, O, N_2^+, O_2^+, NO^+, N^+, O^+, and e^-). They are not of importance in the nonequilibrium flows arising during reentry because the very high temperatures are typically associated with a low degree of dissociation and ionization.

Reentry Applications

The influence of the transport coefficient modeling on nonequilibrium forebody flows and surface heat fluxes was investigated in detail for two different reentry missions. As a typical example for a reentry from low Earth orbit (LEO) with a velocity of $v \approx 7.5$ km/s, the MIRKA reentry capsule was chosen. MIRKA was a German reentry experiment (sphere, 1 m in diameter) which was flown in October 1997 (Refs. 23 and 24). Because of the moderate reentry velocity, the ionization degree does not exceed 0.1%, whereas oxygen is completely dissociated. An example for a high-velocity reentry is the STARDUST reentry flight. STARDUST is a NASA comet sample return capsule that will enter the Earth's atmosphere in 2006 with a velocity of about 13 km/s. Therefore, not only will the temperatures be much higher compared to a LEO reentry, but also the ionization degree will exceed 20%. The flow conditions of the investigated trajectory points are summarized in Table 1.

The flowfields were computed with the URANUS nonequilibrium code[25] using the radiation equilibrium surface assumption. The two-dimensional URANUS nonequilibrium code consists of 18 differential equations. There are 10 species conservation equations for N_2, O_2, NO, N, O, N_2^+, O_2^+, NO^+, N^+, and O^+. There are two momentum conservation equations and six energy conservation equations for the total energy; the vibrational energies of N_2, O_2, and NO; the rotational energy of the molecules; and the translational energy of the electrons. The equations are solved fully coupled and fully implicit. All of the computations were performed on shock-adapted structured grids with a mesh spacing of the order of the local mean free path at the surface. The MIRKA grid consists of 60×52 cells, the STARDUST meshes consist of 55×90 cells for flow case 2 and of 80×90 cells for flow case 3, respectively. The boundary layers are resolved with 28 mesh points in the MIRKA case, up to 38 mesh points in the STARDUST flow case 3. Hence, a sufficient resolution of the forebody flows is assured.

We begin the discussion of the influence of transport coefficient modeling on postshock relaxation with STARDUST (flow case 2). Figures 3 and 4 show temperatures and mole fractions vs stagnation line. When comparing computed temperatures and molar fractions in the postshock relaxation region, it can be observed that the simplified model of Yos[9] leads to a larger relaxation time compared to the first approximation of Chapman and Cowling. Because of the higher diffusion velocities of the Chapman–Cowling approximations, a

Table 1 Investigated test conditions[a]

	Vehicle (flow case)		
Parameter	MIRKA (1)	STARDUST (2)	STARDUST (3)
H, km	56.2	83.7	58.7
ρ_∞, kg/m^3	$5.0 \cdot 10^{-4}$	$1.0 \cdot 10^{-5}$	$3.7 \cdot 10^{-4}$
v_∞, km/s	6.6	11.7	11
Ionization deg, %	$\approx$0.1	$\approx$1	$>$10
$\dot{q}_{St,CC,nc}$, kW/m^2	671	2070	4986
$(\dot{q}_{St,YG,nc} - \dot{q}_{St,CC,nc})/\dot{q}_{St,CC,nc}$, %	−8.7	−6.4	+7.1
$(\dot{q}_{St,YC,nc} - \dot{q}_{St,CC,nc})/\dot{q}_{St,CC,nc}$, %	+1.0	−1.4	−3.6
$\dot{q}_{St,CC,fc}$, kW/m^2	1874	3181	12614
$(\dot{q}_{St,YG,fc} - \dot{q}_{St,CC,fc})/\dot{q}_{St,CC,fc}$, %	−11.7	−7.1	−13.14
$(\dot{q}_{St,YC,fc} - \dot{q}_{St,CC,fc})/\dot{q}_{St,CC,fc}$, %	+0.7	+0.1	−3.7

[a]Influence of transport coefficient models on stagnation point heat fluxes (St) for weakly and strongly ionized flows; fully catalytic (fc) and noncatalytic (nc) radiation equilibrium boundary conditions.

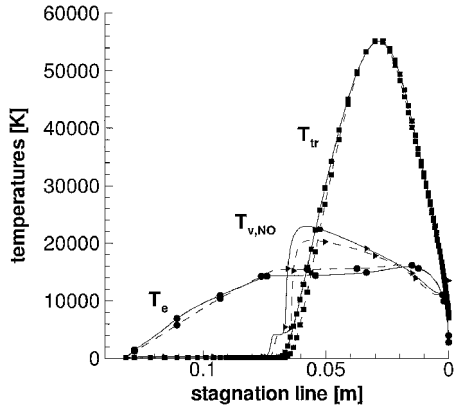

Fig. 3 Selected temperatures for STARDUST reentry at 83.7-km altitude vs stagnation line for different transport coefficient models: dashed line, Yos's model[9] (see also Ref. 4); and solid line, present model (in both cases the collision integrals of Capitelli et al.[10] were used to compute the transport coefficients).

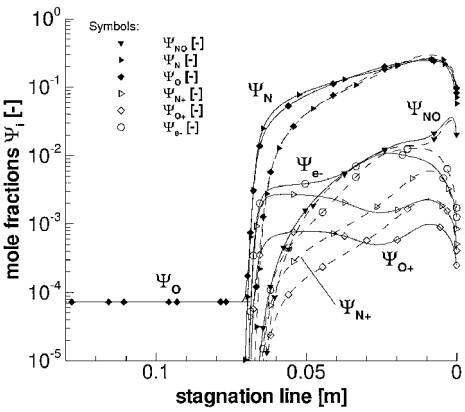

Fig. 4 Selected mole fractions for STARDUST reentry at 83.7-km altitude vs stagnation line for different transport coefficient models: dashed line, Yos's model[9] (see also Ref. 4); and solid line, present model (in both cases the collision integrals of Capitelli et al.[10] were used to compute the transport coefficients).

larger amount of highly excited particles formed during the postshock relaxation moves upstream and increases the reaction probability. The coupling with the coupled vibration–chemistry–vibration thermochemical relaxation model[2] leads to a higher NO vibrational temperature in the vicinity of the shock compared to the flowfield simulation with the simplified transport coefficient model. An influence of heat conduction and viscosity on the shock structure has not been observed. Similar observations can be made for the other two flow cases as well.

Because of the higher upstream density in flow cases 1 and 3, an equilibrium region forms between the postshock relaxation region and the boundary layer. Therefore, the postshock relaxation region is much smaller than in flow case 2. The properties in the equilibrium region are determined by inviscid fluxes and the chemical equilibrium constants. Differences due to viscous transport phenomena could not be observed. Hence, gas-phase composition and temperatures at the boundary-layer edge are not affected by transport coefficients in the flow cases 1 and 3. Next, the influence of transport coefficient modeling on the boundary-layer flow will be discussed. The near surface boundary layer is strongly affected by surface catalycity. Therefore, the three flow cases have been computed with the two limiting assumptions of a noncatalytic and fully catalytic surface. In the case of a noncatalytic surface, no recombination takes place at the surface such that the diffusion fluxes vanish at the surface. In turn, energy transport caused by temperature gradients is the main energy transport mechanism toward the surface. A fully catalytic surface is characterized by the assumption that all heavy particles impinging on the surface (NO, N, O, N_2^+, O_2^+, NO^+, N^+, and O^+) recombine to N_2 and O_2. Therefore, the two energy transport processes are coupled in the vicinity of the surface: Heat conduction as well as transport of chemical energy due to species mass diffusion are the dominant energy transport processes toward the surface. We begin the comparison of the viscous transport phenomena for the different flow cases for a noncatalytic surface. For MIRKA (flow case 1) the heat conductivities computed with both transport coefficient models agree well. Therefore, the computed surface heat fluxes differ by not more than 1% (see Table 1). This is due to the negligible ionization degree and the unchanged boundary-layer edge temperature of about 6000 K. However, note that for the same flow case the collision integrals of Capitelli et al.[10] (CC) lead to about 12% higher heat fluxes than YG, as can be seen from Fig. 5. The STARDUST reentry flow conditions at the altitude $H = 58.7$ km (flow case 3) result in a 23% ionization degree and a boundary-layer edge temperature of about $T \approx 11{,}500$ K. As can be seen from Table 1, the simple model (YC) results in a 3.6% lower stagnation point heat flux than the present model (CC), which leads to $\dot{q}_{W,St} = 5.0$ MW/m^2 if the surface is assumed to be noncatalytic. This difference is caused by the lower electron thermal conductivity and the lower diffusion velocities of the ionized species computed with the Yos's[9] model. Because of the higher heavy particle translational thermal conductivity, the Gupta et al.[4] model (YG) leads to a 7.1% higher stagnation point heat flux than CC.

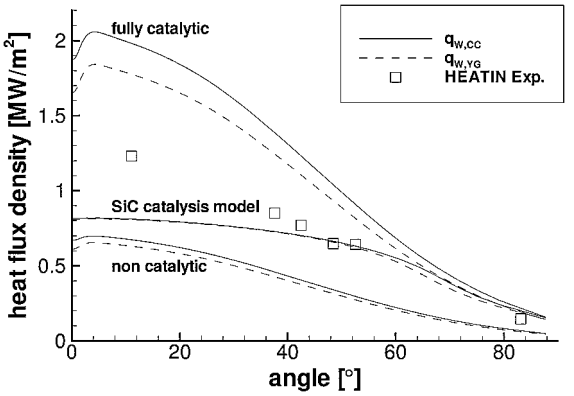

Fig. 5 Influence of transport coefficients onto surface heat fluxes for thermal protection system (TPS) materials of different catalycity during MIRKA reentry at 60-km altitude: dashed line, Gupta et al. model[4]; and solid line, Chapman–Cowling first approximation as presented.

In the case of a fully catalytic surface, the heat flux toward the surface is determined not only by thermal conduction but also by the enthalpy flux due to mass diffusion. As before, the differences caused by the different collision integrals are quite large. The Yos's[9] model leads to a 1% higher stagnation point heat flux for the MIRKA flow case than the present model if the Capitelli et al.[10] collision integrals are used to compute the transport coefficients. This is an effect of the slightly higher diffusion velocities of oxygen and nitrogen computed with effective diffusion coefficients. For the highly ionized STARDUST flow case 3, the diffusion velocities of ions and electron thermal conductivity computed with Yos's[9] model are too small. Therefore, the simplified model (YC) predicts a 3.7% lower stagnation point heat flux than the present model (CC). The computed stagnation point surface heat flux is 13.1% smaller if the simplified model is used together with the Gupta et al.[4] collision integrals.

The influence of transport coefficient models on STARDUST surface heat fluxes at $H = 83.7$ km altitude (flow case 2) is more complicated. Because the entire forebody flow is characterized by chemical and thermal nonequilibrium, the postshock relaxation influences the boundary-layer edge conditions. As can be seen from Fig. 3, the boundary-layer edge translational temperature exceeds 10,000 K by far. Therefore, a significant influence of the transport coefficient model on the surface conditions should be expected. However, a comparison of the simplified model's results (YC) with

Table 2 Benchmark results on different computer architectures[a]

	Yos[9]	CC with D_m	CC
Intel Pentium 200 (CISC Personal Computer)	8.5 s	14.4 s	38.9 s
IBM RS/6000-560 (RISC Workstation)	5.4 s	10.1 s	25.9 s
NEC SX-4/32 (parallel vector supercomputer)	0.134 s	0.195 s	0.999 s

[a]Here 100 loops with a vector length of 100 elements have been timed.

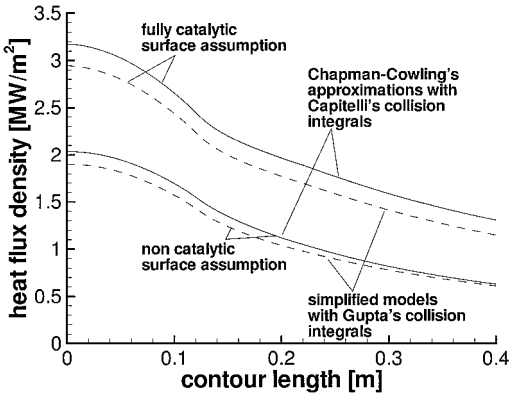

Fig. 6 Influence of transport coefficients on surface heat fluxes for TPS materials of different catalycity during STARDUST reentry at 83.7-km altitude: dashed line, Gupta et al. model[4]; and solid line, Chapman–Cowling first approximation as presented.

the ones of the present model (CC) shows that the stagnation point surface heat fluxes differ by less than 2%. Similar to the other flow conditions, the Gupta et al.[4] collision integrals result in about 7% lower stagnation point surface heat flux than the ones of Capitelli et al.,[10] as can be seen from Fig. 6.

The comparisons made show that the influence of the more accurate transport coefficient model on the surface heat flux of a reentry vehicle is negligible if the ionization degree at the boundary-layer edge is low. Even if the ionization degree at the boundary-layer edge is high, the influence of the transport coefficient model on the surface heat flux is rather small. However, the collision integrals used in the computations have a significant influence on surface heat fluxes.

Benchmarks

As has been shown in the preceding sections, the influence of the transport coefficients on the aerothermal loads on the surface of a reentry vehicle is only weak in dissociated air flows. Therefore, the additional computational work needed to compute the more accurate transport coefficients may be a criterion to decide whether the Chapman–Cowling approximations should be used or not. Table 2 shows benchmark results on different computer architectures. In either case, the different transport coefficients were computed 10,000 times (100 loops with 100 independent mesh points). The column titled Yos[9] shows the benchmark results for the simplified model with the collision integrals given by Gupta et al.[4] The results in the following column show the benchmark results with the first approximations to the viscosity and the thermal conductivity together with effective diffusion fluxes. In the last column the multicomponent diffusion fluxes were computed instead of the effective ones. The results show that up to 7.5 times more time is required to compute the first approximation to the transport coefficients. The approximations to the viscosity and the thermal conductivy used herein can be evaluated without pivoting, and, therefore, only a small amount of additional computational work is needed. Unfortunately, the solution of Eq. (18) requires full pivoting, which prevents vectorization of the algorithm.

Conclusions

A new transport coefficient model based on the first approximation of the Chapman–Cowling theory for multicomponent mixtures[12] is implemented into the URANUS Navier–Stokes code to compute the viscous transport phenomena in high-temperature flows more accurately. The assumptions necessary to obtain the simplified models of Yos[9] and Gupta et al.[4] have been discussed in detail because this model is widely used in current nonequilibrium air Navier–Stokes calculations. The underlying collision integrals were updated to improve the computed transport coefficients.

The transport coefficients computed with both methods differ by up to a factor of two in the case of partially ionized air under equilibrium conditions. Hence, the new model predicts significantly faster thermochemical relaxations in the near shock region of partially ionized reentry nonequilibrium flows. Applying the more accurate transport coefficients in boundary layers at cold vehicle surfaces leads to surface heat fluxes that differ up to 4% from those that are computed with the simplified transport coefficient models.

References

[1]Knab, O., Frühauf, H.-H., and Messerschmid, E. W., "Theory and Validation of the Physically Consistent Coupled Vibration–Chemistry–Vibration Model," *Journal of Thermophysics and Heat Transfer*, Vol. 9, No. 2, 1995, pp. 219–226.

[2]Kanne, S., Knab, O., Frühauf, H.-H., Pogosbekian, M., and Losev, S. A., "Calibration of the CVCV-Model Against Quasi-Classical Trajectory Calculations," AIAA Paper 97-2557, 1997.

[3]Daiß, A., Frühauf, H.-H., and Messerschmid, E. W., "Modeling of Catalytic Reactions on Silica Surfaces with Consideration of Slip Effects," *Journal of Thermophysics and Heat Transfer*, Vol. 11, July 1997.

[4]Gupta, R. N., Lee, K. P., Thomson, R. A., and Yos, J. M., "A Review of Reaction Rates and Transport Properties for an 11-Species Air Model for Chemical and Thermal Nonequilibrium Calculations to 30000 K," NASA TM 85820, 1990.

[5]Daiß, A., Schöll, E., Frühauf, H.-H. and Knab, O., "Validation of the Uranus Navier–Stokes Code for High-Temperature Nonequilibrium Flows," AIAA Paper 93-5070, 1993.

[6]Frühauf, H.-H., "Computation of High-Temperature Nonequilibrium Flows," *Molecular Physics and Hypersonic Flows*, edited by M. Capitelli, NATO ASI Series, Kluwer, Dordrecht, The Netherlands, 1995.

[7]Devoto, R. S., "Transport Properties of Ionized Monatomic Gases," *Physics of Fluids*, Vol. 9, June 1966, pp. 1230–1240.

[8]Devoto, R. S., "Simplified Expressions for the Transport Properties of Ionized Monatomic Gases," *Physics of Fluids*, Vol. 10, Oct. 1967, pp. 2101–2112.

[9]Yos, J. M., "Transport Properties of Nitrogen, Hydrogen, Oxygen and Air to 30,000 K," TR AD-TM-63-7, Research and Advanced Development Div., AVCO Corp., 1963.

[10]Capitelli, M., Gorse, C., Longo, S., and Giordano, D., "Transport Coefficients of High-Temperature Air Species," AIAA Paper 98-2936, June 1998.

[11]Mason, E. A., Munn, R. J., and Smith, F. J., "Transport Coefficients of Ionized Gases," *Physics of Fluids*, Vol. 10, Aug. 1967, pp. 1827–1832.

[12]Hirschfelder, J. O., Curtiss, C. F., and Bird, R. B., *Molecular Theory of Gases and Liquids*, Wiley, New York, 1954.

[13]Ramshaw, J. D., and Chang, C. H., "Ambipolar Diffusion in Two-Temperature Multicomponent Plasmas," *Plasma Chemistry and Plasma Processing*, Vol. 13, No. 3, 1993, pp. 489–498.

[14]Lee, J.-H., "Basic Governing Equations for the Flight Regimes of Aeroassisted Orbital Transfer Vehicles," Progress in Astronautics and Aeronautics, Vol. 96, AIAA, New York, 1985, pp. 3–53.

[15]Sutton, A., and Gnoffo, P. A., "Multicomponent Diffusion with Application to Computational Aerothermodynamics," AIAA Paper 98-2575, 1998.

[16]Vincenti, W. G., and Kruger, C. H., *Introduction to Physical Gas Dynamics*, Wiley, New York, 1965.

[17]Brokaw, R. S., "Approximate Formula for the Viscosity and Thermal Conductivity of Gas Mixtures," *Journal of Chemical Physics*, Vol. 29, Aug. 1958, pp. 391–397.

[18]Pascal, S., and Brun, R., "Transport Properties of Nonequilibrium Gas Mixtures," *Physical Review E*, Vol. 47, May 1993, pp. 3251–3267.

[19]Gmelin, L., *Gmelin—Handbuch der anorganischen Chemie, System Nr. 3 , Sauerstoff*, Verlag Chemie GmbH, Weinheim/Bergstraße, Germany, 1950 (in German).

[20]Devoto, R. S., Bauder, U. H., Cailletteau, J., and Shires, E., "Air Transport Coefficients from Electric Arc Measurements," *Physics of Fluids*, Vol. 21, April 1978, pp. 552–558.

[21]Bacri, J., and Raffanel, S., "Calculation of Transport Coefficients of Air Plasmas," *Plasma Chemistry and Plasma Processing*, Vol. 9, No. 1, 1989, pp. 133–154.

[22]Murphy, A. B., and Arundell, C. J., "Transport Coefficients of Air, Argon–Air, Nitrogen–Air, Oxygen–Air Plasmas," *Plasma Chemistry and Plasma Processing*, Vol. 15, No. 2, 1995, pp. 279–307.

[23]Auweter-Kurtz, M., Burkhardt, J., Fertig, M., Frühauf, H.-H., Habiger, H., Jahn, G., Messerschmid, E. W., and Schöttle, U., "Flugdatenauswertung der MIRKA-Experimente HEATIN und PYREX," *Proceedings der DGLR Jahrestagung*, Dentsche Gesellschaft für Luft- und Raumfahrt, Germany, 1998 (in German).

[24]Fertig, M., and Frühauf, H.-H., "Detailed Computation of the Aerothermodynamic Loads of the MIRKA Capsule," *Proceedings of the Third European Symposium on Aerothermodynamics for Space Vehicles*, European Space Research and Technology Centre, ESA Noordwijk, The Netherlands, 1998.

[25]Frühauf, H.-H., Fertig, M., Olawsky, F., and Bönisch, T., "Upwind Relaxation Algorithm for Reentry Nonequilibrium Flows," *High Performance Computing in Science and Engineering 99*, Springer-Verlag, Berlin, 2000.